Iron Catalysts Reactivation for Efficient CVD Growth of SWNT with Base-growth Mode on Surface

Maoshuai He, Xiaojie Duan, Xuan Wang, Jin Zhang,* Zhongfan Liu,* and Colin Robinson†

Center for Nanoscale Science and Technology (CNST), College of Chemistry & Molecular Engineering, Peking University, Beijing 100871, P. R. China, and Division of Oral Biology, University of Leeds, Clarendon Way, Leeds LS2 9LU, United Kingdom

Received: March 9, 2004

We report here a simple approach to reactivation of iron catalysts for improving the efficiency of catalyst-directed surface growth of SWNTs by heating treatment (normally at 450 °C for 30 min in air). The heat treatment approach can burn off the amorphous carbon coated on catalysts and may change the interaction between the catalysts and substrate, thus reactivating the catalyst for the further growth of SWNTs. It is revealed that the growth efficiency can be greatly enhanced by this multitime growth and that, finally, a much higher growth efficiency of SWNTs may be attained. Furthermore, by using the SWNTs grown on silica surfaces at the first time as a reference, we looked at subsequent growth after heat treatment and obtained the direct experiment evidence of base-growth mode. This approach will provide a useful way to directly control and monitor SWNT growth.

Since their discovery in 1991,[1] the past decade has witnessed significant progress in both the production of carbon nanotubes[2] and their application in a wide variety of fields.[3] Despite this, methods for single-walled carbon nanotubes (SWNTs) production, especially for efficient growth, remain complex and difficult. To make progress in this direction, detailed understanding of growth mechanisms is required. This would not only improve growth efficiency but also would facilitate mass production of well-characterized products. Recently, the successful controlled growth of SWNTs directly on solid surfaces[4−6] by chemical vapor deposition (CVD) has attracted much attention. This approach provides a means of controlling SWNTs growth in terms of efficiency and in terms of the characteristics of the product. In this paper, we report a simple approach to improving the efficiency of catalyst directed surface growth of SWNTs that also permits direct investigation of the growth process.

Catalyst efficiency is often affected by surface poisoning during the growth of carbon nanotubes.[7] The strategy presented here for reactivating catalysts poisoned in this way is shown in Scheme 1. An $Fe(OH)_3$ colloid, prepared by hydrolysis of anhydrous ferric chloride,[8] was dispersed onto a 600-nm thick SiO_2-coated silicon substrate by spin coating at 3000 rpm. The $Fe(OH)_3$-coated SiO_2 substrates were then heated in air at 600 °C to generate ferric oxide nanoparticle catalysts for growth of SWNTs by CVD. This was carried out at 900 °C for 10 min under a flow of CH_4 at 600 standard cubic centimeter per minute (sccm). However, growth efficiency in terms of the ratio of SWNTs to the catalyst particles on the substrate was not high (∼1:20). Examination of the catalyst surface suggested that this was due to coating of some catalyst nanoparticles by amorphous carbon. Using a simple heat treatment at 450 °C for 30 min in air, it proved possible to burn off this amorphous carbon and reactivate the nanoparticle catalyst, generating further growth of SWNTs. Furthermore, by using the SWNTs produced at the first time as a reference, it was possible to investigate the SWNTs growth process after removal of amorphous carbon.

The morphologies and diameter of the as-synthesized nanotubes were characterized by Atomic Force Microscopy (AFM, Digital Instrument, Nanoscope III) and Raman spectroscopy (Renishaw 1000, He−Ne laser excitation wavelength of 632.8 nm). Energy-disperse X-ray analysis (EDAX, FEI Tecnai F30 FEG operated at 300KV) was used to investigate the structure and composition of nanoparticles.

Initial studies have indicated that a key factor in the efficient growth of SWNTs on surfaces via CVD is the presence on the surface of a monodisperse layer of catalytic nanoparticles.[4−7] To achieve this, we have also devised a method of producing $Fe(OH)_3$ colloids by hydrolysis of anhydrous ferric chloride. These colloids were used to produce discrete nanoparticles of ferric oxide with a uniform size distribution on SiO_2 surfaces (Figure 1a). The diameter distribution of the catalytic nanoparticles showed a peak centered at 1.8 nm with 93% in the range $1 \sim 5$ nm (Figure 1b). Only a small proportion of nanoparticles had diameters of ∼7 nm, probably resulting from aggregation during the preparation of Fe $(OH)_3$.

Using these iron-containing catalyst nanoparticles, SWNTs were successfully produced on SiO_2 surfaces. A typical AFM image is shown in Figure 1c; the reaction were carried out at 900 °C for 10 min with $CH_4 = 600$ sccm. The length of the SWNTs ranged from a few hundred nanometers to several microns. The diameter distribution of SWNTs showed a peak centered at 1.6 nm (Figure 1e). These data were also confirmed by Raman spectroscopy. A typical Raman spectrum of the SWNTs grown on a silica surface is shown in Figure 1f, in which the peak at 149 cm^{-1} lies in the range of the breathing mode.[9] This proved the existence of SWNTs. RBM peaks that have been observed were in a range from 80 cm^{-1} to 247 cm^{-1}, indicating the diameter range from 1.0 to 3.1 nm ($d = 248\ cm^{-1}$-nm/ω_r).[10] The result is in good agreement with AFM measurements. Disappearance of the D-line[11] in the Raman spectrum

* To whom correspondence should be addressed. Tel & Fax: 00-86-10-6275-7157, E-mail: jzhang@chem.pku.edu.cn, lzf@chem.pku.edu.cn.
† University of Leeds.

10.1021/jp0489471 CCC: $27.50
Published on Web 08/04/2004

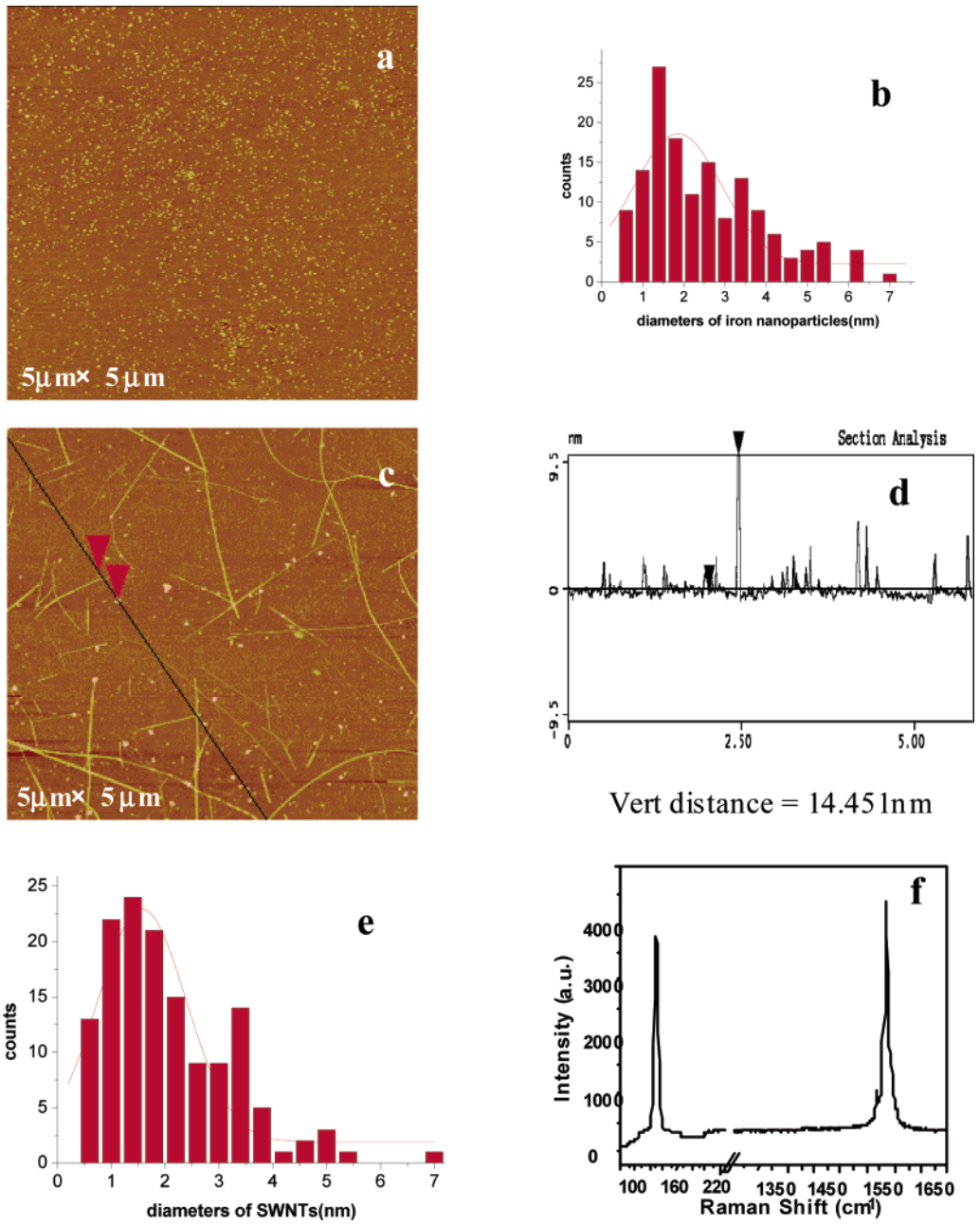

Figure 1. AFM image of SWNTs after calcination at 600 °C in air (a); Histogram of diameter distribution of the catalytic nanoparticles, the mean diameter is 1.8 nm (b); AFM image of carbon nanotubes grown on SiO_2 surface with CH_4 = 600 sccm at 900 °C for 10 min (c); Section analysis of a typical inactive particle (d); Histogram of diameter distribution of the catalytic nanoparticles, the mean diameter is 1.6 nm (e); A typical Raman spectrum of the SWNTs grown on SiO_2 substrates (f).

SCHEME 1: Schematic Illustration of Multitime Growth of SWNTs on SiO_2 Substrates, with Heating in Air. Poisoned Nanoparticles Could be Reactivated and Used for Further Growth of SWNTs

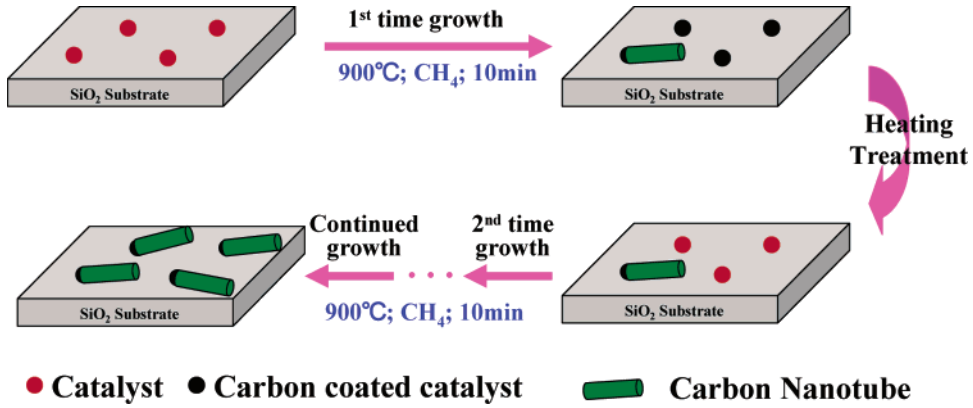

also indicated that high-quality uniform SWNTs were obtained. Consideration of the relationship between catalyst nanoparticle diameter and nanotube diameter revealed that diameters of SWNTs derived from AFM and Raman spectroscopy were a little smaller than that of the catalytic nanoparticles. The reasons for this are not yet clear, but they could be due to some loss of catalyst by evaporation. Of course, there existed a trace amount of nanotubes with a larger diameter (>4 nm) grown on SiO_2; these tubes were double-walled nanotubes (DWNTs) or multi-walled nanotubes (MWNTs) that can be explained by the existence of large catalyst particles.

It was considered that the catalyst particles that had not contributed to the growth of SWNTs had been poisoned during the growth process.[7] Inactivity of some catalyst particles could be explained by the unsuitable interactions between catalytic particles and the silica substrate. Surface roughness of SiO_2 (0.5 nm), for example, might be expected to govern the strength of the interaction between the metal atoms and the substrate. Such factors could determine how the catalyst captures carbon from the gas phase, and how carbon interacts with the catalyst. For instance, the gradient of carbon concentration into the nanoparticle should determine the location from which the SWNTs grow, this will in turn depend on detailed particle−substrate geometry. Examination of the height of poisoned catalyst particle surfaces by AFM indicated that many, but not all, of the inactive catalyst particles were covered by amorphous carbon (Figure 1d). As shown in Figure 1a, few nanoparticles were greater than 7 nm. After the growth of SWNT, however, the diameter of many nanoparticles was greater than 10 nm. Moreover, by prolonging the growth time to 50 min (shown below), the height of many nanoparticles was more than 20 nm, revealing the deposition of more amorphous carbon on the nanoparticles. This was also confirmed by EDAX analysis of inactive catalyst particles. The strong carbon peak appearing in EDAX spectrum indicated that amorphous carbon had deposited on the inactive catalyst (see Supporting Information I).

To eliminate inefficient catalysis due to the build-up of amorphous carbon and, perhaps, unsuitable catalyst substrate interaction, a simple heat/oxidation treatment has been developed. In a typical experiment, after the initial growth of SWNTs the substrate was cooled to room temperature under the protection of Ar, and then heated at 450 °C for 30 min in air. The disappearance of the carbon peak in the EDAX spectrum of the heated individual inactive particle indicated that the amorphous carbon was burned off (see Supporting Information II). Thus, the amorphous carbon-coated nanoparticles would be converted back to ferric oxide. Again, changing the gas environment can alter the strength of the metal−support interaction.[12] Ferric oxide nanoparticles can thus be used for the further growth of SWNTs in the CVD system without additional supplemental catalyst. The AFM imaging (Figure 2a) of catalyst nanoparticles that had not produced SWNTs was repeated after heating in air (Figure 2b). Many of these now showed evidence of SWNT production, indicating that the catalyst had been reactivated. SWNTs grown using reactivated catalyst showed slightly reduced diameters, probably due to some catalyst evaporation. There was little evidence of further growth on already-existing nanotubes. This may offer the possibility of controlling nanotube length by controlling catalyst and growth time.

During the growth of SWNTs on surfaces, at high efficiency, one catalytic nanoparticle should produce one SWNT. Our approach here is an efficient way to maintain catalyst activity and ensure that almost all catalyst particles are effective. By

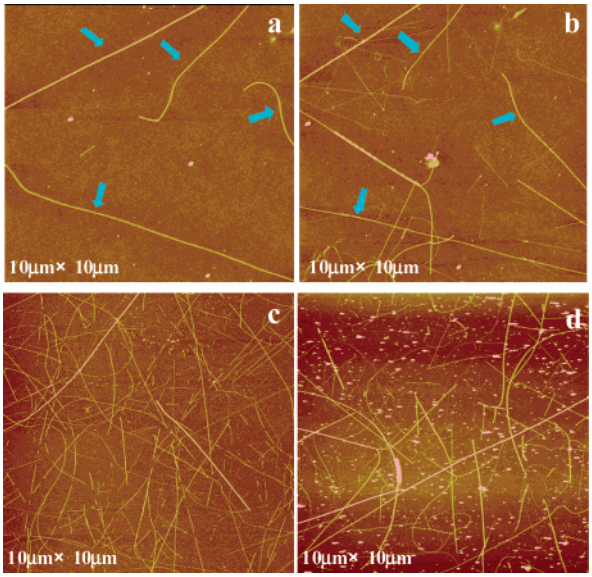

Figure 2. AFM image of SWNTs grown on SiO_2 for 10 min for the first time (a); AFM image of the same area as (a) after the second growth period (b). The arrows indicate the SWNTs grown for the first time; AFM image of carbon nanotubes grown on SiO_2 surface with CH_4 = 600 sccm at 900 °C for 5 × 10 min, alternating with heat treatments in air for 30 min, at 450 °C in every intermission (c); AFM image of carbon nanotubes grown on SiO_2 surface with CH_4 = 600 sccm at 900 °C for 50 min (d).

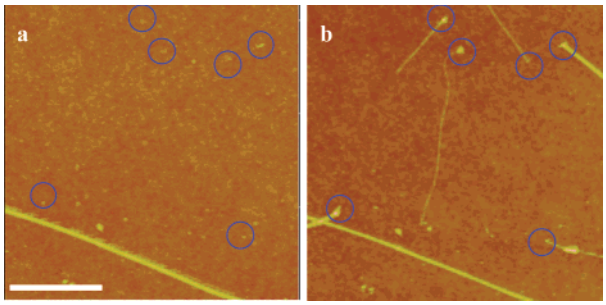

Figure 3. AFM images of the same area after CVD for 10 min (a) and another 10 min (b), confirming the base-growth mode mechanism of SWNTs. During the intermission, heat treatment was done to burn off amorphous carbon. The scale is 1 μm.

using growth times of 5 × 10 min alternating with heat treatments in air for 30 min, at 450 °C, only a few inactive catalytic nanoparticles remained on the substrate (Figure 2c). This was much more efficient than simply lengthening a single initial growth time (Figure 2d). It is revealed that the growth efficiency can be greatly enhanced by this kind of multitime growth. Finally, a much higher growth efficiency of SWNTs may be attained, which is very useful for the site-controlled growth and the designed growth of various nanostructures. Also, as shown in Figure 2d, SWNTs have been grown on SiO_2 substrates for 50 min without intermittence. Section analysis of AFM height measurement on most catalyst nanoparticles showed that their diameter exceeded 20 nm (Supporting Information III). This is further evidence for the coating of amorphous carbon on the particles.

More importantly, using SWNTs grown on silica surfaces in an initial growth phase (as a reference), we were able to use AFM to follow the subsequent growth of SWNTs after further heating cycles and look at the growth mechanism. Comparing the AFM images in the same area of the first (Figure 3a) and second (Figure 3b) growth period, the base-growth mode[13] mechanism of SWNTs on the surface can be clearly demon-

strated. The catalyst nanoparticles were anchored on the substrate and the catalytic nanoparticles did not move (Supporting Information IV). It is suggested that, on the growth surface, the strength of the metal−support interaction can play an important role in modifying the growth characteristics, and that liquid particles are bound to the substrate much more strongly than those in solid state.[14]

In summary, the main results presented in this article are as follows. (1) Discrete iron-containing catalytic nanoparticles of uniform size can be obtained by modified hydrolysis of ferric chloride ($FeCl_3$) and can be used for SWNTs growth. (2) The growth efficiency of catalytic nanoparticles can be greatly improved by a repeated heat treatment in air at 450 °C for 30 min, which reactivates poisoned catalytic nanoparticles. (3) Using the SWNTs first grown on silica surfaces as a reference, we looked at subsequent growth after heat treatment and obtained direct experimental evidence of the base-growth mode. This approach will provide a useful way to control and monitor SWNT growth directly.

Acknowledgment. We are grateful for the financial support from the National Natural Science Foundation of China (NSFC 30000044, 90206023) and the Ministry of Science and Technology of China (2001CB6105).

Supporting Information Available: EDAX spectra of inactive catalyst nanoparticles before(Supporting Information I) and after heat treatment at 450 °C in air (Supporting Information II); Supporting Information III is section analysis of nanoparticles after growth of SWNTs for 50 min; Supporting Information IV is AFM images of nanoparticles on SiO_2 surface at the same area before and after the second growth period without the addition of a carbon source (PDF). This material is available free of charge via the Internet at http://pubs.acs.org

References and Notes

(1) Iijima, S. *Nature* **1991**, *354*, 56.

(2) (a) Bethune, D. S.; Kiag, C. H.; de Vries, M. S.; Gorman, G.; Savoy, R.; Vazquez, J.; Beyers, R. *Nature* **1993**, *363*, 605. (b).Thess, A.; Lee, R.; Nikolaev, P.; Dai, H. J.; Petit, P.; Robert, J.; Xu, C. H.; Lee, Y. H.; Kim, S. G.; Rinzler, A. G.; Colbert, D. T.; Scuseria, G. E.; Tomanek, D.; Fischer, J. E.; Smalley, R. E. *Science* **1996**, *273*, 483. (c) Kong, J.; Soh, H.; Cassell, A.; Quate, C. F.; Dai, H. J. *Nature* **1998**, *395*, 878.

(3) (a) Dai, H. J.; Hafner, J. H.; Rinzler, A. G.; Colbert, D. T.; Smalley, R. E. *Nature* **1996**, *384*, 147. (b) Rueckes, T.; Kim, K.; Joselevich, E.; Tseng, G. Y.; Cheung, C. L.; Lieber, C. M. *Science* **2000**, *289*, 94. (c) Andrews, R.; Jacques, D.; Rao, A. M.; Rantell, T.; et al. *Appl. Phys. Lett.* **1999**, *75*, 1329.

(4) (a) An, L.; Owens, J. M.; McNeil, L. E.; Liu, J. *J. Am. Chem. Soc.* **2002**, *124*, 13688. (b) Huang, S. M.; Cai, X. Y.; Liu, J. *J. Am. Chem. Soc.* **2003**, *125*, 5636.

(5) (a) Cheung, C. L.; Kurtz, A.; Park, H.; Lieber, C. M. *J. Phys. Chem. B* **2002**, *106*, 2429. (b) Joselevich, E. Lieber, C. M. *Nano Lett.* **2002**, *2*, 1137.

(6) (a) Choi, H. C.; Kundaria, S.; Wang, D. V.; Javey, A.; Wang, Q.; Rolandi, M.; Dai, H. J. *Nano Lett.* **2003**, *3*, 157. (b) Ural, A.; Li, Y. M.; Dai, H. J. *Appl. Phys. Lett.* **2002**, *81*, 3464.

(7) Li, Y. M.; Kim, W.; Zhang, Y. G.; Rolandi, M.; Wang, D. V.; Dai, H. J. *J. Phys. Chem. B* **2001**, *105*, 11424.

(8) Meyer, W. R.; Pulcinelli, S. H.; Santilli, C. V.; Craievich, A. F. *J. Non-Cryst. Solids* **2000**, *273*, 41.

(9) (a) Rao, A. M.; Richter, E.; Bandow, S.; Chase, B.; Eklund, P. C.; Williams, K. A.; Fang, S.; Subbaswamy, K. R.; Menon, M.; Thess, A.; Smalley, R. E.; Dresselhaus, G.; Dresselhaus, M. S. *Science* **1997**, *275*, 187. (b) Bandow, S.; Asaka, S.; Saito, Y.; Rao, A. M.; Grigorian, L.; Richter, E.; Eklund, P. C. *Phys. Rev. Lett.* **1998**, *80*, 3779.

(10) Jorio, A.; Saito, R.; Hafner, J. H.; Lieber, C. M.; McClure, T.; Dresselhaus, G.; Dresselhaus, M. S. *Phys. Rev. Lett.* **2001**, *86*, 1118.

(11) Thomsen, C.; Reich, S. *Phys. Rev. Lett.* **2000**, *85*, 5214.

(12) Kukovitsky, E. F.; L'vov, S. G.; Sainov, N. A.; Shustov, V. A.; Chernozatonskii, L. A. *Chem. Phys. Lett.* **2002**, *355*, 497.

(13) (a) Amelinckx, S.; Bernaerts, D.; Zhang, X. B.; Van, G.; Van Landuyt, J. *Science* **1994**, *269*, 1334. (b) Dai, H. J. *Topics Appl. Phys.* **2001**, *80*, 29.

(14) Baker, R. T. K. *Carbon* **1989**, *27*, 315.